Journal of
Water & Climate Change

IWA PUBLISHING

Journal of Water and Climate Change Vol 14 No 7, 2479 doi: 10.2166/wcc.2023.154

Application of GIS using NDVI and LST estimation to measure climate variability-induced drought risk assessment in Ethiopia

Fikiru Temesgen Gelata [a,b], Han Jiqin[a,*], Samerawit Chaka Gemeda[c,d] and Birhan Wubishet Asefa[d]

[a] College of Economics and Management, Nanjing Agricultural University, 210095, Nanjing, Jiangsu, China
[b] Department of Agribusiness and Value Chain Management, Ambo University, 19, Ambo, Ethiopia
[c] Department of Agricultural Economics, Ambo University, 19, Ambo, Ethiopia
[d] Pan African University of Water and Energy Science, including climate change (PAUWES), Tlemcen, Algeria
*Corresponding author. E-mail: jhan@njau.edu.cn

FTG, 0000-0002-2605-8409

ABSTRACT

The contribution of this paper is to assess the drought patterns using the Land Surface Temperature (LST) estimation index and examine the correlation between the Normalized Difference Vegetation Index (NDVI). The main objective was to evaluate the spatiotemporal variation in agricultural drought patterns and severity in order to estimate and measure climate variability. According to the study's findings, the region experienced mild to severe meteorological drought periods 15–18 times over the study period. The majority of these periods (62.72%) were classified as mild drought (unusual dry circumstances), which usually only showed a slight departure from the distribution of rainfall that is close to normal. According to the findings, cropping seasons from 2013 to 2022 saw an increase in agricultural dryness and a decrease in grain yield, with varying degrees of severity in different geographic locations. Based on the result, the major difficulties and challenges identified were the shortage of drinking water, and impacts on air quality, and food and nutrition. Accordingly, agricultural drought risk mapping can be utilized to mitigate the risk associated with drought on agricultural productivity and guide decision-making processes in drought monitoring.

Key words: climate, drought, GIS, LST, NDVI, study areas

HIGHLIGHTS

- Droughts, which are typically associated with high temperatures and low moisture levels, have become increasingly common and critical concerns for all parties involved.
- The unique characterizations for the vegetative area which has an effect on many socioeconomics provided by the remote-sensing-based indices for evaluating the state of vegetation include biomass and growth status.

ABBREVIATIONS AND ACRONYMS

NDVI	Normalized Difference Vegetation Index
MRIS	Moderate Resolution Imaging Spectroradiometer
LST	Land Surface Temperature
SPI	Standardized Precipitation Index
CHIRPS	Climate Hazards Group InfraRed Precipitation with Station
LSBT	Land Surface Brightness Temperature

INTRODUCTION

Drought is a complex natural hazard brought on by climate variability and change that alters the water cycle as a result of precipitation levels lowering sharply over time (Du *et al.* 2013). It has a substantial impact on global food and water security, but how much of an impact relies on our capacity to lower social, economic, and environmental costs (Krishnamurthy *et al.* 2022). The most detrimental natural disaster is drought, which has an effect on many socioeconomic sectors, including

agriculture, ecological services, human health, leisure, and water resources (Smith & Katz 2013). Because it causes water scarcity, agricultural drought, and starvation, drought has the most severe negative consequences on a variety of industries when compared to other natural disasters (Sheffield *et al.* 2018).

Remote sensing is crucial for locating, mapping, assessing, and keeping track of the earth's resources and natural hazards at spatiotemporal scales (Dubovyk 2017). To address and manage the drought situation, numerous techniques and indexes have been developed (Schucknecht *et al.* 2013). Droughts have been more frequent in recent years, and are frequently correlated with high temperatures and low moisture levels. The ecology and human life systems are currently highly vulnerable due to the drought calamity (Yang *et al.* 2021). Therefore, drought needs to be identified using appropriate approaches in order to create accurate temporal continuous mapping (Wijayanti *et al.* 2021). Thus, drought must be specified using formal methods for precise temporal continuous mapping. Geospatial Information System (GIS) can use remote sensing data to estimate the likelihood of drought by providing data on the earth's surface over time (Sur *et al.* 2015). Compared to traditional approaches, remote sensing has improved in mapping the earth's surface, enabling observations and monitoring connected to drought on a temporal and spatial scale (Putri & Nurjani 2018). GIS can make it easier to undertake geographic analyses, such as predicting the likelihood of drought in a region. While some remote sensing methods for tracking droughts have been developed, others have taken the effects of dryness on plants into consideration. One of the oldest vegetation indicators used to track dryness is the Normalized Difference Vegetation Index (NDVI), which has been used since the 1980s (Harun *et al.* 2015).

Numerous studies using the Landsat time-series dataset have been conducted to investigate spatiotemporal patterns of drought, but the majority of those studies focused on drought detection methods and associations between agricultural drought and each rainfall average and crop yield (Van Loon *et al.* 2016). Since they are some of the best at identifying the start of drought and calculating its intensity, length, and global impact, the other studies have published thorough reports on indices that are used to track the impacts of droughts using remote sensing (Liu *et al.* 2018). As a basis for the assessment of vegetation condition, the remote sensing-based indices for assessing the state of vegetation provide distinctive characterizations for the vegetative area, including biomass, growth status, and leaf area coverage (Wan *et al.* 2004). Surface temperature may be a basis for estimating vegetation conditions and evapotranspiration (Liu *et al.* 2018). The performance of drought indices generated based on Moderate Resolution Imaging Spectroradiometer (MRIS) reflectance and Land Surface Temperature (LST), in association with the Standardized Precipitation Index (SPI), was extensively investigated to assess drought conditions on a global to regional scale in the southern Great Plains, USA (Wan *et al.* 2004), China (Du *et al.* 2013), in eastern Africa, and in southern and southeastern Africa (Mutowo & Chikodzi 2014).

The specific objectives of this research are: (i) to assess the drought patterns using the NDVI estimation index; (ii) to assess the drought patterns using the LST estimation index, and (iii) to see the correlation between NDVI and LSTV estimation index at the end of 2022.

METHODOLOGY

Description of the study areas

The study was carried out in the Dire district's Borana Rangeland. The Dire district is located in the southern Borena zone of Ethiopia's Oromia National Regional State, 670 km from Addis Ababa. Bordering Teltele district in the west, Yabelo and Arero in the north-west and north-east, respectively, Borbor in the east northern, and Miyo district in the east, Dire district borders north Kenya in the south (Dinku *et al.* 2018). It occupies an area of 12,722 km^2 and is situated between 3°30′ and 5°00′ N latitude and 37° 30′ to 39° 00′ E longitude (Figure 1). The region is between 688 and 2,480 m above sea level. With a mean annual rainfall of 680–2,000 mm, its bimodal rainfall pattern sees rainfall from April to June and September to November (Demeke *et al.* 2023). This amount of rain is subject to significant seasonal and regional variation (Halounová *et al.* 2011). The district has dry and semi-arid climate conditions. The temperature condition is expressed relative to the evaporation rate in a study that encompasses the entire Zone of Borena, where the Dire district is located, because the evaporation rate in the zone is higher than the precipitation (Demeke *et al.* 2023). A semi-arid climate condition, encompassing the Borena zone, has an average yearly temperature between 18 and 27° (Demeke *et al.* 2023).

Data sources

The NDVI and LST were calculated using remote sensing data from Earth Explorer using Landsat 8 images for the years 2013, 2017, and 2022 for the month of December (LST). The spatially labeled picture file format was used to collect all of the Landsat data. Table 1 details the Landsat acquisition time and related information. The present study's metrological

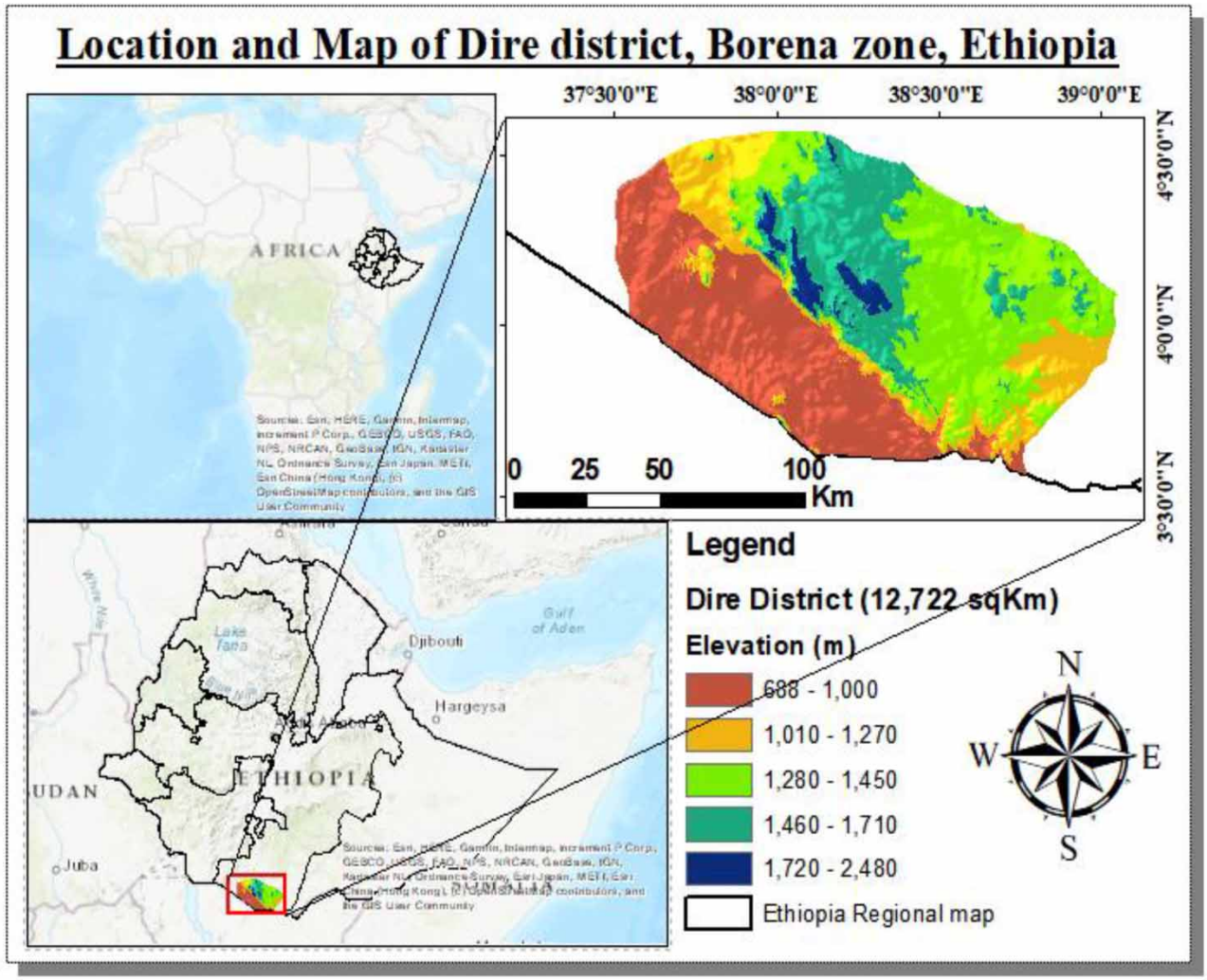

Figure 1 | Description of the study areas.

Table 1 | Specifications of Landsat data used in the study

Activity	Path row	December	Year	Resolution	Cloud cover (%)
Landsat 8	168_57	01	2013	30 m	6
Landsat 8	168_57	12	2017	30 m	6
Landsat 8	168_57	18	2022	30 m	6

data (December rainfall in 2013, 2017, and 2022) were derived from Climate Hazards Group InfraRed Precipitation with Station (CHIRPS) data. This dataset includes gridded rainfall time-series with 0.05° geographic resolution (about 5.3 km) for trend analysis and seasonal drought monitoring.

Data analysis

NDVI estimation

A technique developed in the 1970s and used by earlier investigations was used to determine the NDVI. It included dividing the result by near-infrared radiation after subtracting near-infrared radiation from red radiation (Wolteji *et al.* 2022). The

NDVI's normalized value is always between −1 and +1 (Gebrewahid *et al.* 2017). The ratio of reflected infrared to red wavelength is a superb measure of the health of vegetation. Healthy and densely vegetated areas have a high NDVI value and are less prone to dryness because of their high infrared light reflection and relatively low red light reflectance. A low NDVI score, on the other hand, may indicate a lack of precipitation and stressed vegetation. The NDVI calculation formula is as follows:

$$\mathrm{NDVI} = \frac{(\mathrm{NIR} - \mathrm{R})}{(\mathrm{NIR} + \mathrm{R})} \tag{1}$$

where optical spectrum's near-infrared (NIR) and red (R) bands, respectively. NDVI has a scale of −1 to +1. The typical range of NDVI values for vegetated land is between 0.1 and 0.7, with values greater than 0.5 suggesting healthy vegetation.

LST estimation

In order to determine LST, many parameters must be retrieved. The steps involve applying Equation (2) to convert DN values to radiance values. Then, using temperature constants, the final equation's input for Land Surface Brightness Temperature (LSTB) was derived. Equation (3) was calculated using the NDVI and the amount of vegetation (PV) in Equations (4) and (5) to get the land surface emissivity (LSE). In contrast, LST is the conversion of at-sensor radiance to the top of atmosphere brightness temperature. The outputs then determine the real skin LST (Tang *et al.* 2014) and are calculated as indicated in the equation:

$$L\lambda = \mathrm{ML} * Q_{cal} + \mathrm{AL} - O_i \tag{2}$$

where $L\lambda$ indicates TOA spectral radiance (Watts/(m^2*sr*μm)); ML indicates radiance multiplicative band (No.); AL indicates radiance add band (No.); Q_{cal} indicates quantized and calibrated standard product pixel values (DN); O_i indicates correction for band 10 is 0.29.

Spectral radiance data can be converted to the top of atmosphere brightness temperature using the constant thermal values in a metadata file.

$$\textit{Kelvin}\ (K)\ \textit{to Celsius}\ (^{\circ}C)\ BT = K2/ln(K1/L\lambda + 1) - 273.15 \tag{3}$$

where BT = top of atmosphere brightness temperature (°C); $L\lambda$ = TOA spectral radiance (Watts/(m^2*sr*μm)); $K1 = K1$ constant band (no.); $K2 = K2$ constant band (no.); LSE is the average emissivity of an element on the earth's surface calculated from NDVI values.

$$\mathrm{PV} = \left(\frac{(\mathrm{NDVI} - \mathrm{NDVI_{min}})}{(\mathrm{NDVI_{max}} - \mathrm{NDVI_{min}})}\right)^2 \tag{4}$$

where PV refers to proportion of vegetation; NDVI refers to DN values from the NDVI image; $\mathrm{NDVI_{min}}$ refers to minimum DN values from the NDVI image; $\mathrm{NDVI_{max}}$ refers to maximum DN values from the NDVI image.

$$E = 0.004 \times \mathrm{PV} + 0.986 \tag{5}$$

where E = land surface emissivity; PV = proportion of vegetation, and 0.986 corresponds to a correction of the equation.

The LST is the radiative temperature calculated using the top of atmosphere brightness temperature, wavelength of emitted radiance, and LSE.

RESULTS AND DISCUSSION

Using average annual NDVI, average seasonal NDVI (Figure 2), average yearly VCI, and seasonal VCI and NDVI anomaly for belg, kiremt, and dry season, spatial and temporal variation of agricultural drought patterns and severity were examined. The average annual NDVI, seasonal NDVI, NDVI anomaly, and seasonal VCI were all determined from 2013 to 2022. During the growing season, the same guidelines were followed, first for the belg season (from

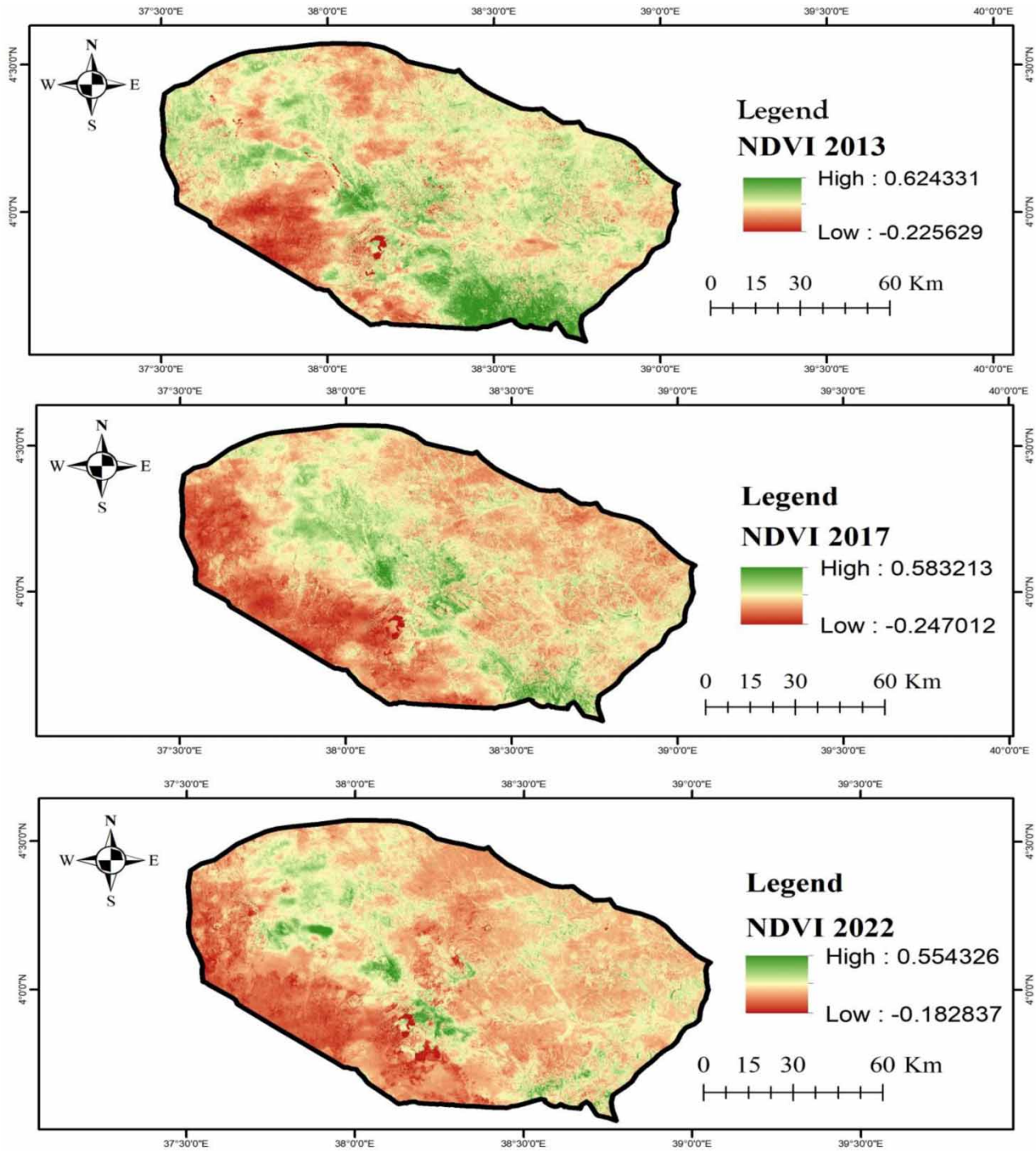

Figure 2 | NDVI result from 2013 to 2022 for December.

March to May) and then for the kiremt season (June to September). The classifications of drought severity for the annual NDVI anomaly, which vary from no drought to mild drought, are illustrated in Figure 2. For the 2003–2017 time period, the VCI-detected lack ranges from no shortage to serious drought. The trend and distribution of LST in the region are shown in Figure 3. The average land and air temperatures for the past seven years are depicted linearly in Figure 3 throughout the course of 8 days. From 2013 through 2022, there is a rising tendency in the early summers, which

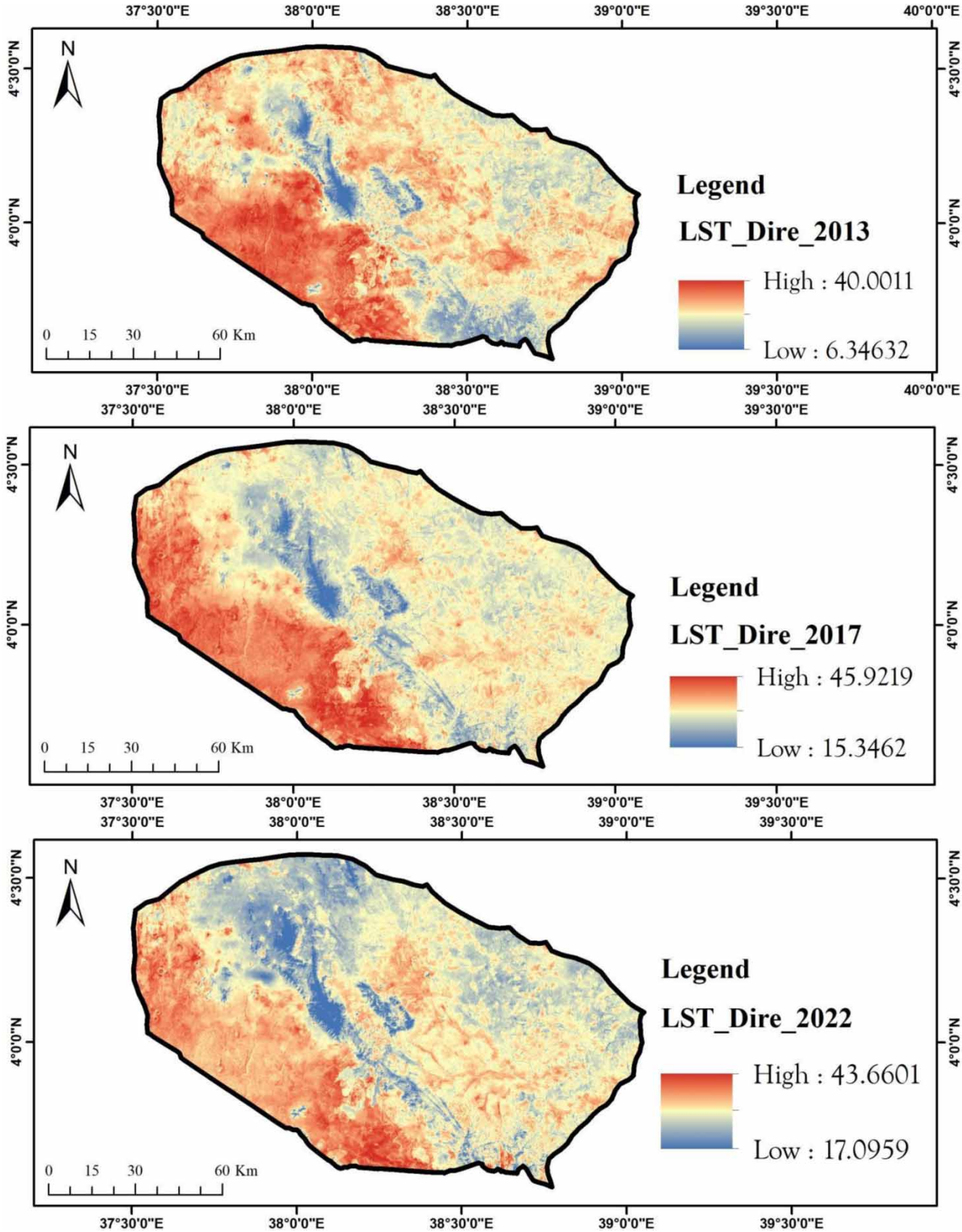

Figure 3 | LST result from 2013 to 2022 for December.

last 76 days from 1 March to 15 May. The LST temperature distribution in boxes and whiskers of Figure 3 serves as a guide for calculating the variance, minimum, mean, and maximum temperature distributions for a period of seven years. LST shows a total temperature range of 52–54 °C from 2013 to 2022, with the most recent year of 2023 showing a maximum LST of 54 °C.

The majority of the LST/NDVI area in 2017 demonstrated evidence of the inverse relationship, which means that as the surface temperature increased, the NDVI value decreased (Figure 4). Less water was left on the soil for plant transpiration, which suggests that the vegetation is under more stress. In dry conditions, rising leaf temperatures are reliable indicators of plant moisture stress and the start of the drought. In 2013, similar behavior was evident (Figure 4). The rising trend of LST in the research areas was significantly influenced by the declining plant cover, expanding built-up area, and increasing impervious surface. The sites with the lowest LST had developed infrastructure, were actively cultivated, or had undeveloped land. This outcome is in line with past study, which found that variations in temperature within cities are caused by variations in inter-urban height (Feyisa *et al.* 2016). Other study researchers discovered employed inferential statistics and mean surface temperatures to assess the effect of land use land cover (LULC) changes on temperature (Dorsey *et al.* 2018). Drought is one of the other climate extremes made worse by LULC changes (Wolteji *et al.* 2022).

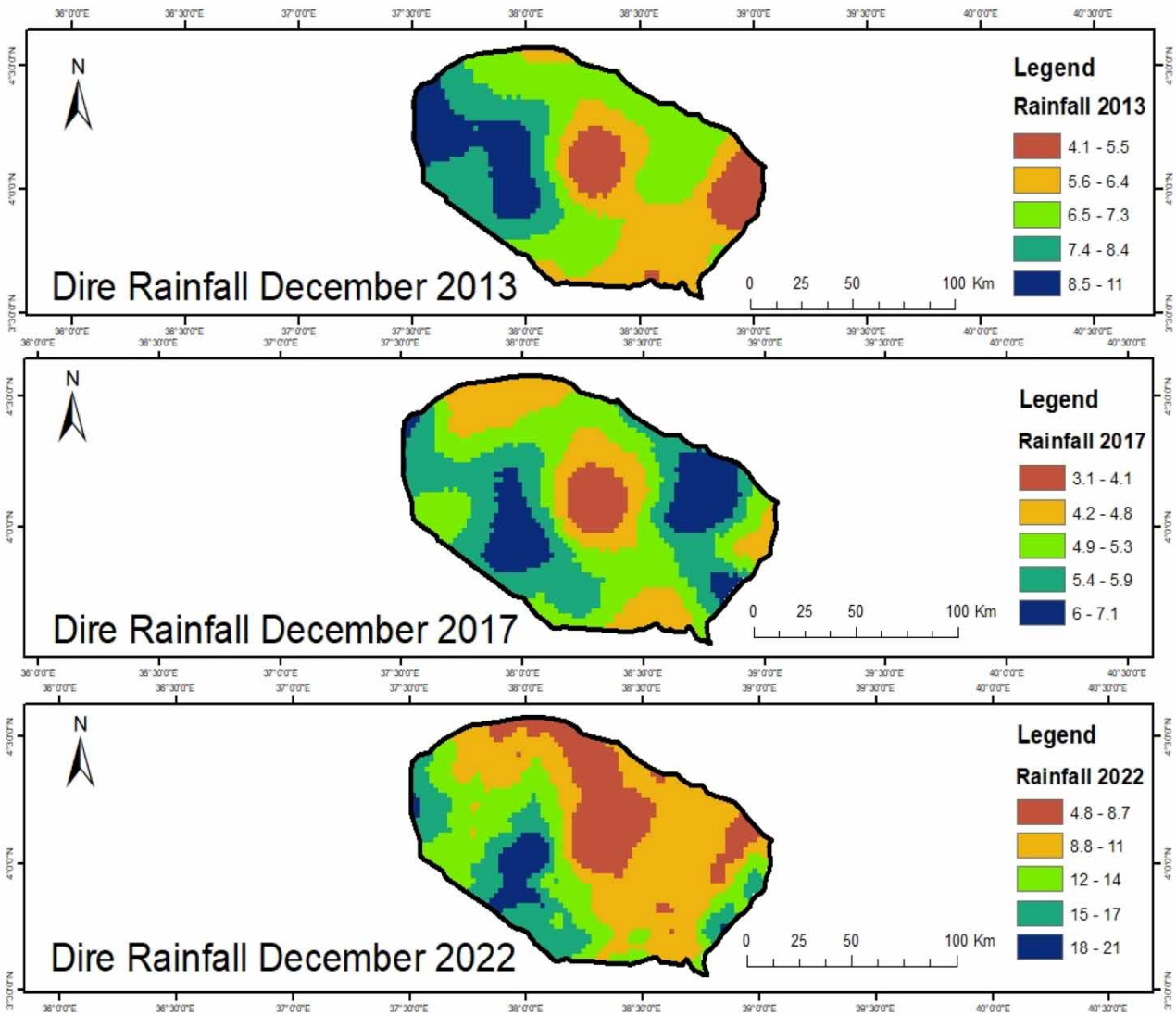

Figure 4 | Precipitation results from 2013 to 2022 for the month of December.

Correlation between LST and NDVI by using PS

A correlation map was made using the NDVI and LST data for December for each of the three years 2013, 2017, and 2022. The NDVI and LST values for the entire research area are correlated in Figure 5. The higher concentration pixels in the scatter plots are represented by the NDVI and LST values. There is an inverse relationship between LST and NVDI which is depicted in correlation coefficient of −0.51 and there is conventionally when one value decreases as the other decreases correlation is negative indicated by Figure 5. Low LST values are easily explained by the fact that high NDVI values are attained because their vegetation is water-limited rather than temperature-limited.

The result of Figure 5 showed a negative association between LST and NDVI when energy is the limiting factor for vegetation development, which is the case at higher latitudes and elevations in the research area. In contrast, during the middle of the growing season, solar radiation less impacts the LST–NDVI correlation's nature since the radioactive flux throughout most of the study region is high enough not to restrict vegetation development. According to the result, the LST–NDVI correlations are typically negative throughout this sub-period except for the northernmost parts. Based on the

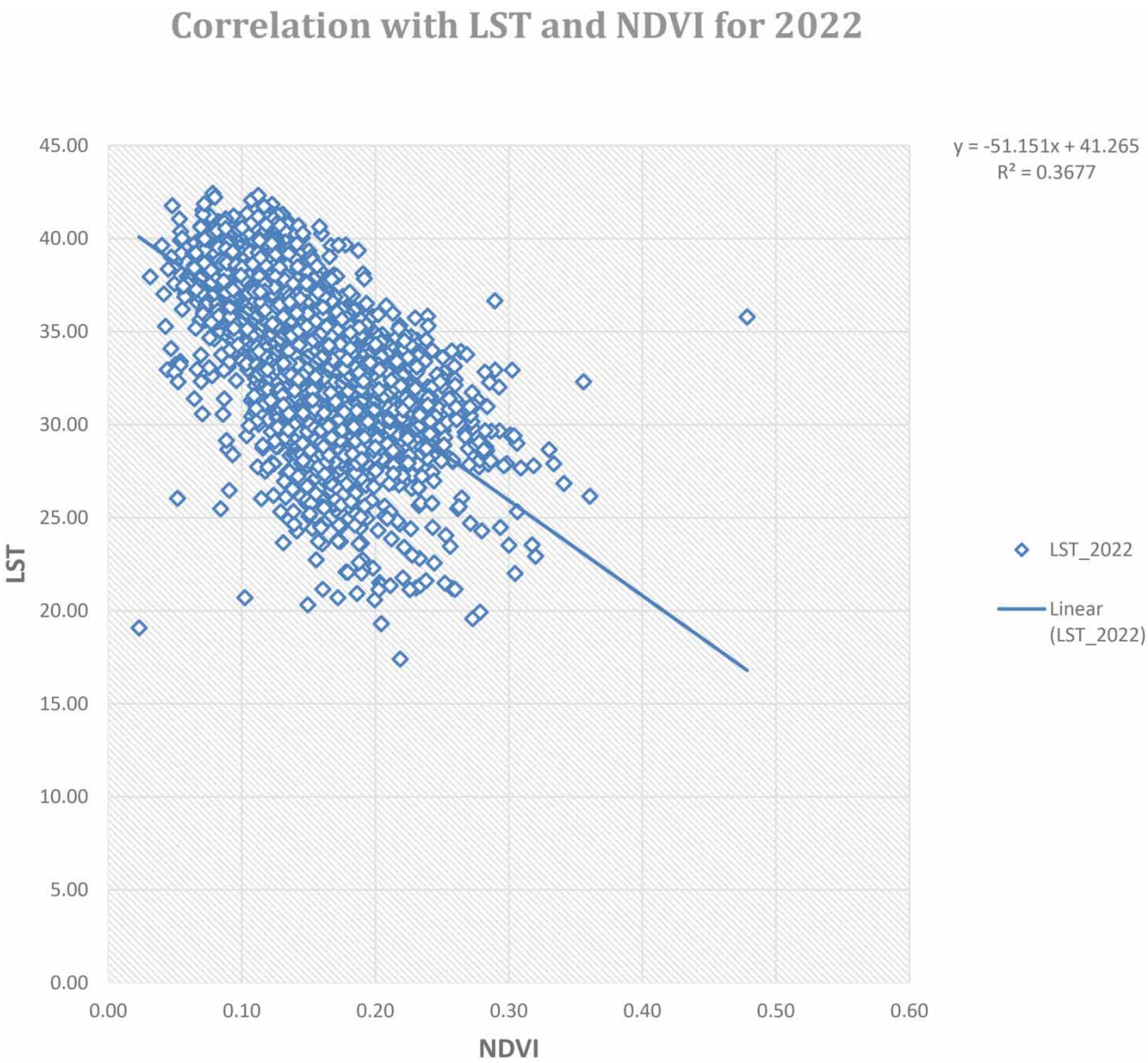

Figure 5 | The correlation between LST and NDVI 2022.

result, as anticipated, the slope progressively changes from negative to positive from the south to the north. The correlations at the four main sites along this transect were determined to be inconsequential, and significant negative correlations were only observed at the two southernmost points.

Discussion

The frequency of droughts in the study area was prepared using a GIS map of historical drought intensity. The results confirmed that there was intricate regional heterogeneity in the frequency of drought episodes in the region. This shows that at least 15 rainfall deficiencies occurred in every district in the area. Over the course of the study period, the area experienced mild to severe meteorological drought periods 15–18 times. The majority of it (62.72%) occurred during a mild drought (abnormally dry conditions), which typically only showed a little departure from the distribution of rainfall that is close to normal. However, because of how this lack of rain affects vegetation growth, it frequently results in agricultural droughts that are brought on by high LST intensities which were supported by the findings of Sahana *et al.* (2021).

For the sake of the environment and the quality of life for those who live in rural regions, it is crucial to investigate the rate of LST in response to LULC change. It is important to look into how much rural life has changed for both urban residents and biodiversity. It is crucial to look at the rate of LST in response to LULC change for the sake of the environment and the standard of living for those who reside in rural areas. Examining how rural life has changed is essential to safeguarding biodiversity and urban people as highly related with the findings of Band *et al.* (2022). It is claimed that the increase in NDBI and LST during the research period was brought on by the loss in plant cover that was identified by the NDVI. Critical scholars highlighted the LST and NDVI's inverse linear relationship (Sahana *et al.* 2021). LST, on the other hand, enjoys a positive connection. The other researcher found that NDBI and LST have a positive relationship (Band *et al.* 2022).

Drought is a complicated natural event that can lead to reduced water supply, which can have a substantial impact on agriculture and economic activities and cause social dissatisfaction and political instability. Based on the result, drought indicators are used to pinpoint insufficiencies that was supported by the study findings of Shamshirband *et al.* (2020). This study looked into the use of the NDVI and LST data from Terra-MODIS to see if a method for monitoring drought in close to real-time would be useful (Marengo *et al.* 2009). This technique is known as the Vegetation Supply Water Index (VSWI), which takes into account thermal properties and land surface reflectance which was related to the findings of Shamshirband *et al.* (2020).

According to the data, a severe drought afflicted approximately 85% of the Borana semi-arid region between 2013 and 2022. The number of days of soil moisture deficit, computed with a simple water balance model and daily interpolated precipitation, was used to confirm the results (Sahana *et al.* 2021). According to a correlation analysis of Vermont Significant Wetland Inventory, precipitation, and soil moisture deficit, VSWI is closely related to rainfall and soil water content, especially in dry conditions, which proposes adopting VSWI as a strategy for drought monitoring in the near real-time (Band *et al.* 2022). In the analysis of the 2013–2022 droughts using the VSWI index, two crucial features of vegetation's response to drought conditions – vegetation's recovery and memory impacts – were brought to light.

CONCLUSION

Regarding its usefulness for drought monitoring, this study investigates the geographical and temporal relationship between LST and NDVI and its correlation in Ethiopia. This study aimed to use the remote sensing-based VSWI to explore the spatial and temporal aspects of vegetative drought in the study areas. According to the findings, it is possible to use the empirical LST–NDVI relationship as a reliable predictor of the geographical and temporal aspects of water stress situations in the studied areas. The 2013 and 2022 droughts impacted vegetated regions (crop/pasture), which the VSWI index successfully recognized. According to the study, locations outside the semi-arid boundary also experienced drought during the 2012–2013 droughts, even though the semi-arid zone is more susceptible to drought stress conditions. Monitoring results from indicators frequently differ due to the various information sources and principles used for drought indices. It can be seen that no one index is adequate for accurately capturing drought features. As a result, using multiple indicators simultaneously or using indices combining data from multiple sources may produce results closer to reality. This finding suggests that drought behavior is highly erratic. This has significant implications for planners and policymakers who are actively involved in drought mitigation and preparedness.

ACKNOWLEDGMENT

The authors acknowledge the research fund sponsorship of "the Projects of institute local cooperation of Chinese Academy of Engineering, grant number JS2020ZT12" and "Priority Academic Program Development of Jiangsu Higher Education Institutions Project (PAPD)'.

DATA AVAILABILITY STATEMENT

All relevant data are included in the paper or its Supplementary Information.

CONFLICT OF INTEREST

The authors declare there is no conflict.

REFERENCES

Band, S. S., Karami, H., Jeong, Y.-W., Moslemzadeh, M., Farzin, S., Chau, K.-W., Bateni, S. M. & Mosavi, A. 2022 Evaluation of time series models in simulating different monthly scales of drought index for improving their forecast accuracy. *Frontiers in Earth Science* **10**, 839527.

Demeke, B., Dejene, T. & Abebe, D. 2023 Genetic variability, heritability, and genetic advance of morphological, yield related and quality traits in upland rice (Oryza Sativa L.) genotypes at pawe, northwestern Ethiopia. *Cogent Food & Agriculture* **9** (1), 2157099.

Dinku, T., Funk, C., Peterson, P., Maidment, R., Tadesse, T., Gadain, H. & Ceccato, P. 2018 Validation of the CHIRPS satellite rainfall estimates over Eastern Africa. *Quarterly Journal of the Royal Meteorological Society* **144**, 292–312.

Dorsey, E. R., Elbaz, A., Nichols, E., Abbasi, N., Abd-Allah, F., Abdelalim, A., Adsuar, J. C., Ansha, M. G., Brayne, C., Choi, J.-Y. J., Collado-Mateo, D., Dahodwala, N., Do, H. P., Edessa, D., Endres, M., Fereshtehneiad, S.-M., Foreman, K. J., Gankpe, F. G., Gupta, R., Hamidi, S., Hankey, G. J., Hay, S. I., Hegazy, M. I., Hibstu, D. T., Kasaeian, A., Khader, Y., Khalil, I., Khang, Y.-H., Kim, Y. J., Kokubo, Y., Logroscino, G., Massano, J., Ibrahim, N. M., Mohammed, M. A., Mohammadi, A., Moradi-Lakeh, M., Naghavi, M., Nguyen, B. T., Nirayo, Y. L., Ogbo, F. A., Owolabi, M. O., Pereira, D. M., Postma, M. J., Oorbani, M., Rahman, M. A., Roba, K. T., Safari, H., Safiri, S., Satpathy, M., Sawhney, M., Shafieesabet, A., Shiferaw, M. S., Smith, M., Szoeke, C. E. I., Tabares-Seisdedos, R., Truong, N. T., Ukwaja, K. N., Venketasubramanian, N., Villafaina, S., Weldegwergs, K. G., Westerman, R., Wijeratne, T., Winkler, A. S., Xuan, B. T., Yonemoto, N., Feigin, V. L., Vos, T. & Murray, C. J. L. 2018 Global, regional, and national burden of Parkinson's disease, 1990–2016: a systematic analysis for the global burden of disease study 2016. *The Lancet Neurology* **17** (11), 939–953.

Du, L., Tian, Q., Yu, T., Meng, Q., Jancso, T., Udvardy, P. & Huang, Y. 2013 A comprehensive drought monitoring method integrating MODIS and TRMM data. *International Journal of Applied Earth Observation and Geoinformation* **23**, 245–253.

Dubovyk, O. 2017 The role of remote sensing in land degradation assessments: opportunities and challenges. *European Journal of Remote Sensing* **50** (1), 601–613.

Feyisa, G. L., Meilby, H., Jenerette, G. D. & Pauliet, S. 2016 Locally optimized separability enhancement indices for urban land cover mapping: exploring thermal environmental consequences of rapid urbanization in Addis Ababa, Ethiopia. *Remote Sensing of Environment* **175**, 14–31.

Gebrewahid, T. W., Yao, Z.-J., Yan, X.-C., Gao, P. & Li, Z.-F. 2017 Identification of leaf rust resistance genes in Chinese common wheat cultivars. *Plant Disease* **101** (10), 1729–1737.

Halounová, L., Vepřek, K. & Řehák, M. 2011 Geographic Information System Models of 40-Year Spatial Development of Towns in the Czech Republic. In: *The Third International Conference on Advanced Geographic Information Systems, Applications, and Services, GEOProcessing.*

Harun, R., Muresan, I. C., Arion, F. H., Dumitras, D. E. & Lile, R. 2015 Analysis of factors that influence the willingness to pay for irrigation water in the Kurdistan Regional Government, Iraq. *Sustainability* **7** (7), 9574–9586.

Krishnamurthy, R. P. K., Fisher, J. B., Choularton, R. J. & Kareiva, P. M. 2022 Anticipating drought-related food security changes. *Nature Sustainability* **5** (11), 956–964.

Liu, K., Su, H., Tian, J., Li, X., Wang, W., Yang, L. & Liang, H. 2018 Assessing a scheme of spatial-temporal thermal remote-sensing sharpening for estimating regional evapotranspiration. *International Journal of Remote Sensing* **39** (10), 3111–3137.

Marengo, J. A., Schaeffer, R., Pinto, H. & Zee, D. 2009 *Mudanças Climáticas E Eventos Extremos no Brasil*. FBDS, Rio de Janeiro.

Mutowo, G. & Chikodzi, D. 2014 Remote sensing based drought monitoring in Zimbabwe. *Disaster Prevention and Management* **23**, 649–659.

Putri, I. I. & Nurjani, E. 2018 Persepsi dan Adaptasi Petani Padi Lahan Kering di Klaten Terhadap Variabilitas Curah Hujan. *Jurnal Bumi Indonesia* **7** (3), 97–114.

Sahana, V., Mondal, A. & Sreekumar, P. 2021 Drought vulnerability and risk assessment in India: sensitivity analysis and comparison of aggregation techniques. *Journal of Environmental Management* **299**, 113689.

Schucknecht, A., Erasmi, S., Niemeyer, I. & Matschullat, J. 2013 Assessing vegetation variability and trends in north-eastern Brazil using AVHRR and MODIS NDVI time series. *European Journal of Remote Sensing* **46** (1), 40–59.

Shamshirband, S., Hashemi, S., Salimi, H., Samadianfard, S., Asadi, E., Shadkani, S., Kargar, K., Mosavi, M., Nabipour, N. & Chau, K.-W. 2020 Predicting standardized streamflow index for hydrological drought using machine learning models. *Engineering Applications of Computational Fluid Mechanics* **14** (1), 339–350.

Sheffield, J., Wood, E. F., Pan, M., Beck, H., Coccia, G., Serrat-Capdevila, A. & Verbist, K. 2018 Satellite remote sensing for water resources management: potential for supporting sustainable development in data-poor regions. *Water Resources Research* **54** (12), 9724–9758.

Smith, A. B. & Katz, R. W. 2013 US billion-dollar weather and climate disasters: data sources, trends, accuracy and biases. *Natural Hazards* **67** (2), 387–410.

Sur, C., Hur, J., Kim, K., Choi, W. & Choi, M. 2015 An evaluation of satellite-based drought indices on a regional scale. *International Journal of Remote Sensing* **36** (22), 5593–5612.

Tang, L., Yang, X., Yin, Q., Cai, K., Wang, H., Chaudhury, I., Yao, C., Zhou, Q., Kwon, M., Hartman, J. A., Dobrucki, I. T., Dobrucki, L. W., Borst, L. B., Lezmi, S., Helferich, W. G., Ferguson, A. L., Fan, T. M. & Cheng, J. 2014 Investigating the optimal size of anticancer nanomedicine. *Proceedings of the National Academy of Sciences* **111** (43), 15344–15349.

Van Loon, A. F., Gleeson, T., Clark, J., Van Dijk, A. I., Stahl, K., Hannaford, J., Di Baldassarre, G., Teuling, A. J., Tallaksen, L. M., Uijlenhoet, R., Hannah, D. M., Sheffield, J., Svoboda, M., Verbeiren, B., Wagener, T., Rangecroft, S., Wanders, N. & Van Lanen, H. A. J. 2016 Drought in the Anthropocene. *Nature Geoscience* **9** (2), 89–91.

Wan, Z., Wang, P. & Li, X. 2004 Using MODIS land surface temperature and normalized difference vegetation index products for monitoring drought in the southern Great Plains, USA. *International Journal of Remote Sensing* **25** (1), 61–72.

Wijayanti, R., Jaelani, L., Handayani, H. & Chu, H. 2021 Drought index mapping in Java Island using sentinel-3 SLSTR. *International Journal of Geoinformatics* **17** (4), 97–108.

Wolteji, B. N., Bedhadha, S. T., Gebre, S. L., Alemayehu, E. & Gemeda, D. O. 2022 Multiple indices based agricultural drought assessment in the Rift valley region of Ethiopia. *Environmental Challenges* **7**, 100488.

Yang, J., Ren, J., Sun, D., Xiao, X., Xia, J. C., Jin, C. & Li, X. 2021 Understanding land surface temperature impact factors based on local climate zones. *Sustainable Cities and Society* **69**, 102818.

First received 30 March 2023; accepted in revised form 7 June 2023. Available online 22 June 2023